Draft version December 30, 2017
Preprint typeset using LaTeX style emulateapj v. 12/16/11

SYNCHROTRON EMISSION FROM KNOTS OF EXTENDED JETS

Samaresh Mondal, Partha Pratim Basumallick, Nayantara Gupta
Astronomy and Astrophysics Group, Raman Research Institute, C.V. Raman Avenue, Sadashivanagar, Bangalore 560080, India
Draft version December 30, 2017

ABSTRACT

Radio observations by ALMA and upper limits on gamma ray flux by Fermi LAT have ruled out inverse Compton scattering of Cosmic Microwave Background radiation by relativistic electrons (IC/CMB) as the origin of X-ray emission from extended jets of six quasars 3C 273, PKS 0637-752, PKS 1136-135, PKS 1229-021, PKS 1354+195, and PKS 2209+080. Previously it has been shown that proton synchrotron could be the possible radiative process for X-ray emission from the extended jets of 3C 273 and PKS 0637-752. Here we extend this study to include five other extended jets of quasars S5 2007+777, PKS 1136-135, PKS 1229-021, PKS 1354+195, and PKS 2209+080 to find out whether their X-ray emission could be of proton synchrotron origin. Each extended jet contains several knots distributed along its length, which are emitting brightly in radio to X-ray frequencies. We model the emission from each knot separately to study whether there are knot to knot variations in the strength of magnetic field, luminosity in relativistic electrons and protons.

Keywords: quasars:general; X-rays:galaxies; gamma-rays:galaxies

1. INTRODUCTION

Several extended jets of distant quasars have been observed in radio frequencies by Atacama Large Millimeter/submillimeter Array (ALMA), in optical frequencies by Hubble Space Telescope (HST), in X-rays by Chandra X-ray observatory and in gamma rays by Fermi LAT. In most cases we only have upper limits on gamma ray fluxes. The multi-wavelength emission from kilo-parsec scale jets is most often explained by synchrotron emission of relativistic electrons in radio and optical frequencies, and inverse Compton scattering of Cosmic Microwave Background (CMB) radiation by relativistic electrons (IC/CMB) in X-ray frequencies (Tavecchio et al. 2000; Celotti et al. 2001; Sambruna et al. 2008). For some of the newly discovered extended jets the X-ray emission could be explained satisfactorily with IC/CMB model (Simionescu et al. 2016; Zacharias & Wagner 2016).

With the latest observational data covering from radio to gamma ray frequencies our understanding of radiative emission from extended jets is changing drastically. The gamma ray flux expected from IC/CMB model exceeds the upper limits from Fermi LAT in some of the cases (Meyer & Georganopoulos 2014; Meyer et al. 2015, 2017), thus ruling out this model. IC/CMB model of X-ray emission has been ruled out for the extended jets of 3C 273 (Meyer & Georganopoulos 2014), PKS 0637-752 (Meyer et al. 2015, 2017) and more recently for the extended jets of some other quasars PKS 1136-135, PKS 1229-021, PKS 1354+195, and PKS 2209+080 (Breiding et al. 2017).

Other scenarios of multi-wavelength photon emission from the extended jets could be two populations of electrons emitting synchrotron emission in different frequency ranges (radio and X-rays) or relativistic electrons emitting synchrotron emission in radio frequencies and relativistic protons in X-ray frequencies. It is difficult to explain physically how there could be two populations of electrons accelerated within the extended jets. The alternative scenario of proton synchrotron emission could be possible as protons lose energy very slowly by synchrotron emission and traverse long distances before cooling down. Proton synchrotron model has been applied to the extended jet of 3C 273 and PKS 0637-752 in earlier works (Kundu & Gupta 2014; Bhattacharyya & Gupta 2016; Basumallick & Gupta 2017). The magnetic field needed to explain the X-ray emission in the proton synchrotron model is of mG order for 3C 273 and PKS 0637-752. Most of the jet luminosity is due to this strong magnetic field. The Lorentz factor of the emission region could be close to 3 in the proton synchrotron model, which is physically plausible as a kilo-parsec scale jet is expected to move much slower than a parsec scale jet.

Here we apply the proton synchrotron model to the extended jets of S5 2007+777, PKS 1136-135, PKS 1229-021, PKS 1354+195, and PKS 2209+080. The modelling is done using the code by (Krawczynski et al. 2004). We fit the radio and X-ray data for each knot separately to find out the values of the physical parameters for each knot. In section 2 we discuss about the model used in our study and describe each of the quasar extended jets considered in our work. The same model has been applied to the knots of each of the extended jets. Our detailed study on the applicability of proton synchrotron model would be helpful to rule out this model in several cases and indicate the need for alternative innovative scenarios to understand the emission mechanisms in extended jets.

Our results are discussed in section 3 and conclusion is drawn based on these results in section 4.

2. SYNCHROTRON MODELLING OF SPECTRAL ENERGY DISTRIBUTIONS (SEDS)

Shock accelerated electrons and protons in the knots are losing energy in the magnetic field by synchrotron radiations. The energy density in the magnetic field is more than in the CMB photons, hence IC/CMB of electrons is not important in this case. A break appears E_{el}^{brk} in the power law spectrum of electrons due to cooling. The

smondal@camk.edu.pl

synchrotron cooling time scale is

$$t^{el}_{synch} = \frac{\gamma_{el} m_{el} c^2}{\frac{4}{3}\sigma^{el}_{Th} c U_B \gamma^2_{el} \beta^2_{el}} sec \quad (1)$$

σ^{el}_{th} is Thomson cross-section and $U_B = \frac{B^2}{8\pi}$ is the magnetic energy density. The electrons are relativistic with dimensionless speed $\beta_{el} \approx 1$. The age of the extended jet t_{jet} may be in the range of $10^5 - 10^7$ years (Basumallick & Gupta 2017). In the present work we assume $t_{jet} = 10^6$ years for all the extended jets. The break energy in the electron spectrum is calculated by equating the synchrotron cooling time to the age of the extended jet. The electron spectrum finally used for the calculation of synchrotron emission is

$$\frac{dN_{el}(E_{el})}{dE_{el}} = A \begin{cases} E^{-p_1}_{el} & E_{el} < E^{brk}_{el} \\ E^{brk}_{el} E^{-p_2}_{el} & E_{el} > E^{brk}_{el} \end{cases} \quad (2)$$

'A' is a normalisation constant. p_1 and p_2 are spectral indices below and above break energy E^{brk}_{el} respectively, for synchrotron cooling $p_2 = p_1 + 1$.

Similarly for the shock accelerated relativistic protons we assume a power law spectrum and the break energy is calculated by comparing the time scales of diffusion and synchrotron loss to the age of the jet. The Bohm diffusion time scale for the protons is

$$t_{diff} \simeq 4.2 \times 10^5 \eta^{-1} B_{mG} R^2_{kpc} (E/10^{19} eV)^{-1} years. \quad (3)$$

where R_{kpc} is the size of the region in kilo-parsec. The acceleration and emission region is assumed to be a spherical blob of radius R. The constant factor η is assumed to be 1, magnetic field $B_{mG} = \frac{B}{10^3} G$. The synchrotron energy loss time scale for relativistic protons is given by

$$t_{synch} = 1.4 \times 10^7 B^{-2}_{mG} (E/10^{19})^{-1} years. \quad (4)$$

Due to the low density of target photons in the kilo-parsec scale jet $p\gamma$ interactions are not important. For the range of the parameter values used in our study the Bohm diffusion time scale is smaller than the synchrotron loss time scale and it is equated to the age of the jet to calculate the break energy in the proton spectrum. The broken power law proton spectrum given below is used to calculate the synchrotron emission which can explain the X-ray data.

$$\frac{dN_p(E_p)}{dE_p} = A \begin{cases} E^{-p_1}_{p} & E_p < E^{brk}_{p} \\ E^{brk(p_2-p_1)}_{p} E^{-p_2}_{p} & E_p > E^{brk}_{p} \end{cases} \quad (5)$$

We note that $p_2 = p_1 + 1$, as the spectrum steepens by $1/E_p$ due to Bohm diffusion losses. Moreover the maximum energy of the protons E^{max}_p is constrained by this relation

$$B \geq 30 \frac{E^{max}_p 10^{15}}{10^{19} R} Gauss. \quad (6)$$

For all the knots in the extended jets of the six quasars we have followed the same method of modelling as discussed above.

The total jet power is calculated using this expression

$$P_{total} = \pi R^2 \Gamma^2 c (u'_B + u'_e + u'_p) \quad (7)$$

where u'_B, u'_e and u'_p are the energy densities in magnetic field, electrons and protons respectively. R is the radius of the spherical emission region moving with Lorentz factor Γ.

S5 2007+777 — The BL Lac object S5 2007+777 at a redshift of 0.342 having hybrid FR I and FR II radio morphology is classified as HYMOR object. The isotropic bolometric luminosity of S5 2007+777 is 5.12×10^{45} erg/sec (Nemmen et al. 2012). The extended jet of S5 2007+777 has five knots $K_{3.6}$, $K_{5.2}$, $K_{8.5}$, $K_{11.1}$ and $K_{15.7}$. The distances of the knots from the core are measured in arcsecs in the 1.49 GHz image of VLA. The radio data from knot $K_{8.5}$ is fitted with electron synchrotron and the X-ray data is fitted by two ways (i) IC/CMB (ii) synchrotron from a second population of electrons (Sambruna et al. 2008). They assumed the jet to be strongly beamed with Doppler factor δ=13. The superluminal feature found in VLBI observation constrains the jet to be aligned within $\sim 24^o$ to our line of sight. Which implies the deprojected length of the jet to be 150 kpc. The jet luminosity required to fit the data in the IC/CMB model is of the order of 10^{46} erg/sec. In our study, we have used viewing angle θ_{obs}=24^o and Lorentz factor Γ=3. The other parameters values have been listed in Table 1. We have modelled the emission from each of the knots separately by electron (lower frequency) and proton synchrotron (higher frequency) assuming the emission region for each knot is a blob of same size. Equipartition is maintained between magnetic field and proton energy densities. All the parameter values of our model for the knots are given Table 1 and Table 2. Fig.1. shows the data points from knots fitted with electron and proton synchrotron emissions. The total jet power required in the extended jets to model the X-ray emission with proton synchrotron model is of the order of 10^{47} erg/sec which is higher than that required in the IC/CMB model.

PKS 1136-135 — The FR II object PKS 1136-135 located at redshift 0.556 has been observed by Hubble Space Telescope and Chandra X-ray observatory (Sambruna et al. 2006). The extended jet of this source has eight knots observed in radio and X-ray frequencies. They used IC/CMB model to fit the X-ray emission from the outer knots and synchrotron emission from a second population of electrons for the inner knots. It is interesting to note that the radio flux increases but the X-ray flux decreases with the distance of the knots from the core. The nearest knot α has the least radio flux and the furthest knot HS has the maximum radio flux. It was suggested that plasma deceleration could be the cause of decrease in the X-ray to radio flux ratio.

The IC/CMB and two population electron synchrotron models were revisited later (Cara et al. 2013). They discussed that IC/CMB model is disfavoured due to the high polarisation in the optical data from the knots. The gamma ray flux expected from IC/CMB exceeds the upper limits from Fermi LAT for the first three knots α, A and B (Breiding et al. 2017). They also noted fitting the UV data with IC/CMB model for knot α and A over predicts the X-ray flux from them. Moreover the UV spectrum is harder than that expected from the IC/CMB model.

We have applied the electron and proton synchrotron model with equipartition in magnetic field and proton energy densities, and a lower value of viewing angle. The Eddington luminosity of PKS 1136-135 is 3.45×10^{46} erg/sec (Liu et al. 2006) is lower than the total jet power required to explain the emission from all the knots in the proton synchrotron model which is 9×10^{47} erg/sec . The values of the parameters used to fit the multi-wavelength data from the knots of PKS 1136-135 are given in Table 3 and Table 4. Fig.2. shows the data points from the knots fitted with our model.

PKS 1229-021— PKS 1229-021 located at a redshift of 1.045 has been observed by Chandra X-ray observatory (Weisskopf et al. 2000) and Hubble Space Telescopre (Tavecchio et al. 2007). VLA image at 8.4GHz frequency shows four knots A, B, C and D. Atacama Large Millimete/submillimeter Array (ALMA) and Chandra have resolved knot A in the extended jet of PKS 1229-021 but the emission from the knots B, C, D could not be resolved separately. More observational data from the separate knots would be helpful to model the spectral energy distributions from each knot separately. The data points shown in Fig.3. have been taken from (Breiding et al. 2017). Eddington luminosity of PKS 1229-021 is 6.31×10^{46}erg/sec (Liu et al. 2006). The values of the parameters used in this work are given in Table 5 and Table 6. In this case also the jet power required in the proton synchrotron model exceeds the Eddington's luminosity of source.

PKS 1354+195— PKS 1354+195 located at redshift 0.72 has a bright core. VLA and ALMA observations resolved two knots A and B in its extended jet. Due to the bright core it is difficult to resolve knot A in X-rays. The X-ray flux from knot B has been used in (Breiding et al. 2017) to infer the X-ray flux from knot A. Its jet emission has been studied by (Sambruna et al. 2002) and (Sambruna et al. 2004) with IC/CMB model. We have taken the observed X-ray flux at 1 KeV from (Sambruna et al. 2004) and other multi-wavelength observational data from (Breiding et al. 2017). The Eddington luminosity of this quasar is $2.93 \times 10^{47} erg/sec$ (Liu et al. 2006). The multi-wavelength data and the fittings of the SEDs are shown in Fig.4. Table 7 and Table 8 display the values of the parameters used in our model. Super-Eddington jet power is required to explain the emission from knot A in the proton synchrotron model.

PKS 2209+080— The object PKS 2209+080 located at redshift 0.485 has five knots A, B, C, D, E in its extended jet. The extended jet emission was modelled with IC/CMB earlier (Jorstad & Marscher 2006). Only one X-ray data point was noted from knot E in this paper. Due to the lack of X-ray data from the knots we can not constrain the values of the model parameters. The radio and optical data are available for all the knots. From electron synchrotron modelling of these data we constrain the magnetic field. We have predicted the possible X-ray flux from the knots in the proton synchrotron model. Future observations with Chandra would be helpful for better understanding of knot emission. The mass of its central blackhole is yet unknown. Assuming it to be $10^9 M_\odot$ the Eddington luminosity is expected to be 1.22×10^{47}erg/sec. Fig.5. shows the observed fluxes and the SEDs from our model. The values of the parameters used in the present work are given in Table 9 and Table 10. The total jet power required in the proton synchrotron model 8.7×10^{47} erg/sec could be lower if the X-ray emission is lower from the knots.

PKS 0637-752— PKS 0637-752 located at a redshift of 0.651 has four knots in its extended jet. IC/CMB model has been ruled out for the jet emission by ALMA data and Fermi LAT upper limits (Meyer et al. 2015, 2017). It has been shown earlier that the X-ray emission from the knots could be explained by proton synchrotron model (Basumallick & Gupta 2017). Here we do a more detailed study including the radio and X-ray data from each of the knots separately and modelling them with electron and proton synchrotron respectively. The magnetic field used in this work is lower than used earlier (Basumallick & Gupta 2017) however the Doppler factor is now slightly higher. The Eddington luminosity of PKS 0637-752 could be of the order of 10^{48} erg/sec (Kusunose & Takahara 2017). The values of the parameters used in our model are displayed in Table 11 and Table 12. The total jet power required is comparable to the Eddington's luminosity of this source. Fig.6. shows the observed fluxes from the knot emissions and the SEDs from our model.

3. RESULTS AND DISCUSSIONS

The SEDs fitted in our model to the data from the knots of the extended jets of six quasars are shown in Fig.1. to Fig.6. Table 1 to Table 12 have the parameter values used to fit the data. In Fig.1. the intensities of radio and X-ray emissions from the knots of S5 2007+777 can not be related to their distances from the core. The brightest knot in radio $K_{8.5}$ is also brightest in X-rays. The magnetic field in the knots is in the range of 1.15 mG to 2 mG. We note that the minimum energy of the relativistic protons are assumed to be high in our model to lower the jet luminosity. The viewing angle of the jet is constrained from radio observations. A smaller viewing angle would lead to a larger Doppler factor and that would reduce the jet power required to explain the X-ray emission with proton synchrotron model.

Fig.2. shows the emissions from the knots of PKS 1136+135. We have many low energy data points from the knots of its extended jet. The radio fluxes from the knots increase with their distances from the core. But a similar variation in the X-ray fluxes from the knots has not been observed. In Table 3 the magnetic field varies in the range of 1 mG to 2 mG. The total jet power required in the knots is much higher than the Eddington luminosity 3.45×10^{46} erg/sec of this source. Equipartition is assumed in the magnetic field and proton energy densities for all the five extended jets in Fig.1. to Fig.5. We do not have observational constraints on the viewing angles for the extended jets of PKS 1136+135, PKS 1229-021, PKS 1354+195, PKS 2209+080 and PKS 0637-752. Low values of the same is assumed to lower the required jet powers.

Fig.3. shows the multi-wavelength emission from knot A and combined emission from knots B, C and D of PKS 1229-021. In future with more observational data it would be possible to study the knot to knot variations of the emissions from B, C and D. The total jet

power required 2×10^{48} erg/sec exceeds the Eddington luminosity 6.31×10^{46} erg/sec of this source. To fit the spectrum from the knots B, C, D a hard spectral index 1.6 is needed. Table 5 shows the magnetic field is slightly higher 4 mG in this case.

The extended jet of PKS 1354+195 has two knots A and B. Fig.4. shows the SEDs of these knots. The knot A nearer to the core is brighter in radio and X-ray frequencies than the knot B. The spectrum is hard for both the knots.

Fig.5. shows the data points and SEDs from the five knots of PKS 2209+080. In future with better observational data in X-ray frequencies the modelling could be improved to constrain the parameter values. The nearest knot is brightest in radio. But the radio fluxes do not decrease systematically with the distances of the knots from the core.

Fig.6. shows the multi-wavelength emissions from the knots of PKS 0637-752. The radio and X-ray fluxes are the least from the nearest knot $WK_{5.7}$. With more observational data in X-ray frequencies the modelling could be improved in future. The total jet power required is comparable to the Eddington's luminosity of the source in this case.

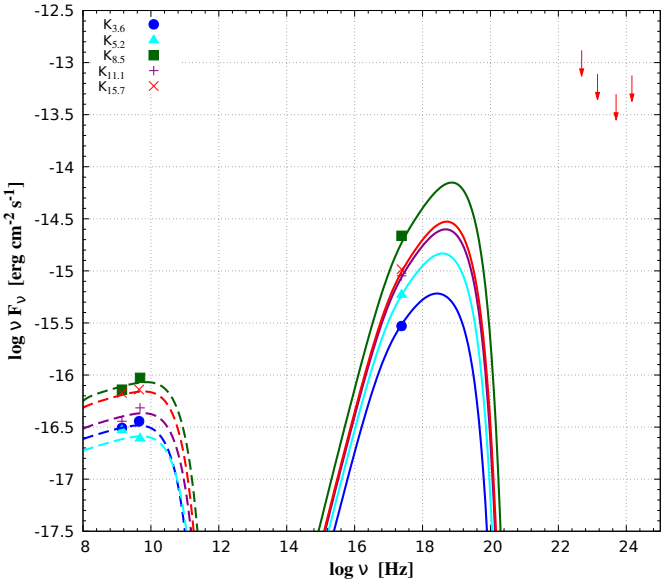

Figure 1. Multi-wavelength data of the knots in the extended jet of S5 2007+777 from (Sambruna et al. 2008). The short dashed line represents electron synchrotron spectrum and the solid line is for proton synchrotron spectrum. Different colours and types of points represent different knots. Fermi LAT upper limits are shown with downward red arrows.

4. CONCLUSION

We have fitted the multi-wavelength data from the knots of the extended jets of the quasars S5 2007+777, PKS 1136-135, PKS 1229-021, PKS 1354+195, PKS 2209+080, PKS 0637-752 with electron and proton synchrotron emissions in the low (radio, optical) and high energy (X-ray) regimes respectively. The radio and X-ray fluxes from the knots do not always vary systematically with their distances from the cores of the quasars. Moreover, the radio and X-ray fluxes could not be correlated in many cases. In most cases the proton synchrotron model requires super-Eddington luminosity although it does not violate the Fermi LAT upper limits. We find the knot emissions from the extended jet of PKS 0637-752 could be explained by the proton synchrotron model which is in agreement with earlier result (Basumallick & Gupta 2017). In case of PKS 1229-021 observed data is not available for the knots B, C and D separately. There is only one X-ray data point from knot E of the extended jet of PKS 2209+080, and no X-ray data is available from the other knots of its extended jet. The Fermi LAT upper limits are useful to constrain the model parameters. In future our model could be tested with more observational data and the values of the model parameters may change, although the conclusion of our study is expected to remain unchanged.

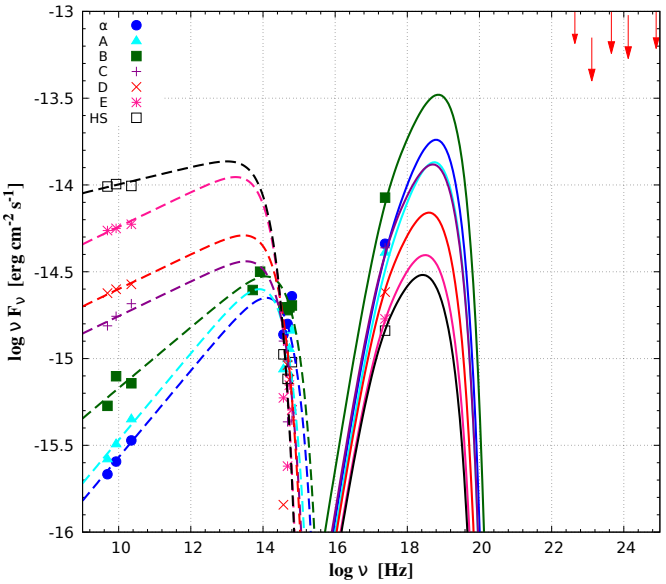

Figure 2. Multi-wavelength data of the knots in the extended jet of PKS 1136-135 from (Sambruna et al. 2006). The data points for wavelengths 555nm, 5.8μm, 3.6μm have been taken from (Breiding et al. 2017). The line styles representing the electron and proton synchrotron emissions are same as in Fig.1. Different colours and types of points are showing the different knots. Red downward arrows represent Fermi LAT upper limits as given in (Breiding et al. 2017).

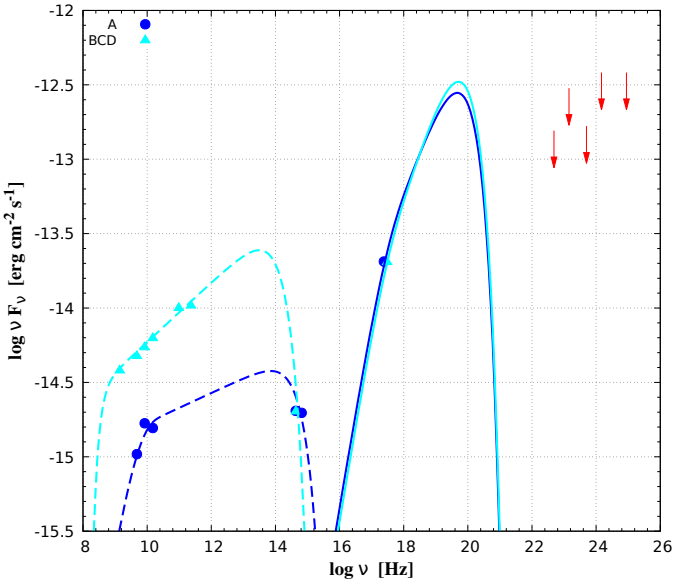

Figure 3. Multi-wavelength data of the knots in the extended jet of PKS 1229-021. Data points have been taken from (Breiding et al. 2017). BCD represents combined flux from knots B, C, D as these knots could not be resolved separately. The line styles representing the electron and proton synchrotron emissions are same as in Fig.1. Different colours and types of points are showing the different knots. Red downward arrow represents Fermi LAT upper limits (Breiding et al. 2017).

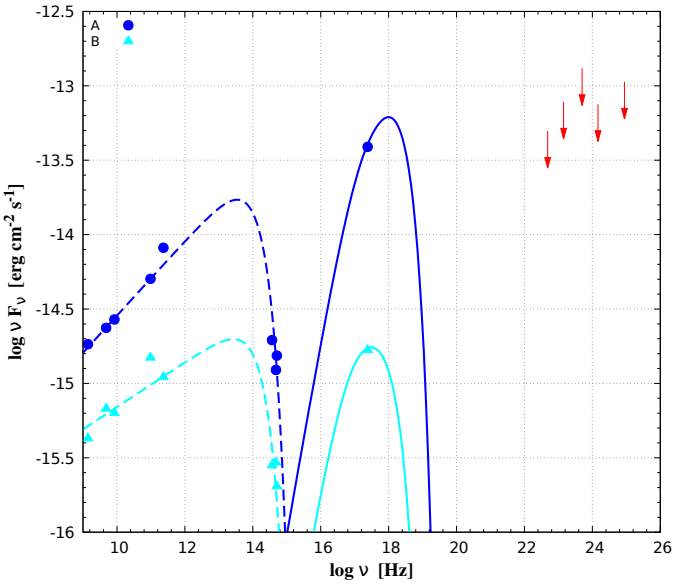

Figure 4. Multi-wavelength data from the knots of the extended jet of PKS 1354+195. Data points and Fermi LAT upper limits have been taken from (Breiding et al. 2017).

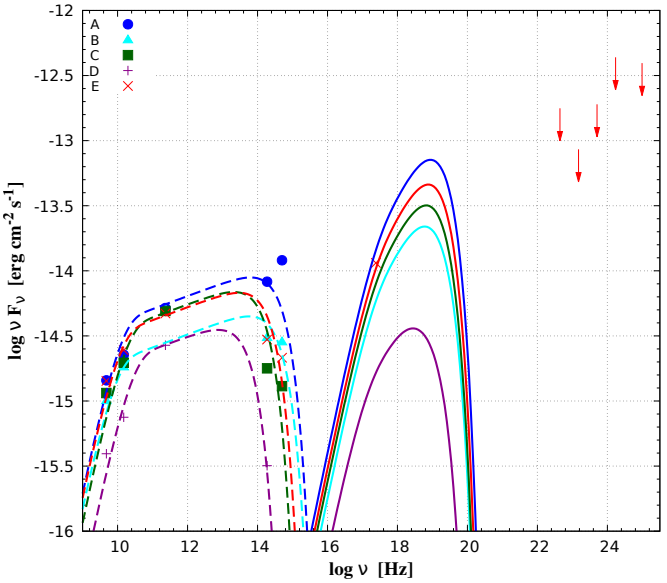

Figure 5. Multi-wavelength data from the five knots of the extended jet of PKS 2209+080. Data points and Fermi LAT upper limits have been taken from (Breiding et al. 2017).

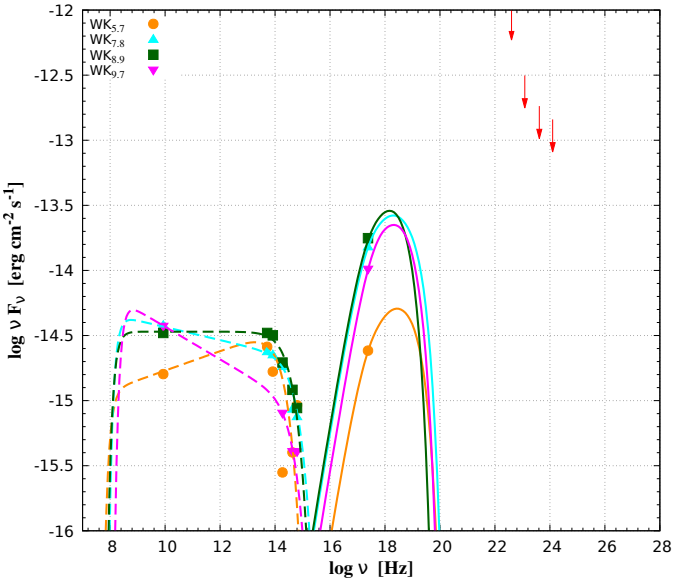

Figure 6. Multi-wavelength data from the knots of the extended jet of PKS 0637-752. Data point have been taken from (Mehta et al. 2009) and Fermi LAT upper limits from (Meyer et al. 2015).

REFERENCES

Bhattacharyya W. and Gupta N., 2016, **ApJ, 817, 121**
Basumallick, P. P. and Gupta, N., 2017,**ApJ, 844, 58**
Breiding, P., Meyer, E. T., Georganopoulos, M., et al., 2017, **ApJ, 849, 95**
Cara, M., Perlman, E. S., Uchiyama, Y., et al., 2013, **ApJ, 773, 186**
Celotti, A., Ghisellini, G. & Chiaberge, M., 2001, **MNRAS, 321, L1**
Kundu, E. and Gupta, N., 2014, **MNRAS, 444, L16**
Jorstad, S. G. & Marscher, A. P., 2006, **Astronomische Nachrichten, 327, 227**
Liu, Y., Jiang, D. R., & Gu, M. F., 2006, **ApJ, 637, 669**

Table 1

Parameters used for modelling multi-wavelength data from extended jet of S5 2007+777 using synchrotron emission model for different knots.

Knots	Dist	Γ	θ_{obs}	δ	$B(mG)$	Emission	$E_{min}eV$	$E_{max}eV$	$E_{break}eV$	p_1	p_2
$K_{3.6}$	$3.6''$	3	24°	2.4	1.15	e^-synch	10^6	10^9	9.33×10^6	1.8	2.8
						p^+synch	10^{17}	1.58×10^{18}	5.01×10^{17}	1.8	2.8
$K_{5.2}$	$5.1''$	3	24°	2.4	1.4	e^-synch	10^6	10^9	6.30×10^6	1.8	2.8
						p^+synch	10^{17}	1.58×10^{18}	6.16×10^{17}	1.8	2.8
$K_{8.5}$	$8.5''$	3	24°	2.4	2	e^-synch	10^6	10^9	3.09×10^6	1.8	2.8
						p^+synch	10^{17}	1.58×10^{18}	8.7×10^{17}	1.8	2.8
$K_{11.1}$	$11''$	3	24°	2.4	1.58	e^-synch	10^6	10^9	4.89×10^6	1.8	2.8
						p^+synch	10^{17}	1.58×10^{18}	6.91×10^{17}	1.8	2.8
$K_{15.7}$	$16''$	3	24°	2.4	1.64	e^-synch	10^6	10^9	4.57×10^6	1.8	2.8
						p^+synch	10^{17}	1.58×10^{18}	7.24×10^{17}	1.8	2.8

Table 2

Particles and magnetic energy densities of different knots and their contribution to jet power for object S5 2007+777

Knots	$u'_B(erg/cm^3)$	R cm	P_B(erg/sec)	Emission	$u'_{part}(erg/cm^3)$	P_{part}(erg/sec)	P_{total}(erg/sec)
$K_{3.6}$	5.26×10^{-8}	10^{21}	4.46×10^{46}	e^-synch	9×10^{-12}	7.63×10^{42}	8.92×10^{46}
				p^+synch	5.26×10^{-8}	4.46×10^{46}	
$K_{5.2}$	7.8×10^{-8}	10^{21}	6.61×10^{46}	e^-synch	6×10^{-12}	5.08×10^{42}	1.32×10^{47}
				p^+synch	7.8×10^{-8}	6.61×10^{46}	
$K_{8.5}$	15.92×10^{-8}	10^{21}	13.5×10^{46}	e^-synch	1.4×10^{-11}	1.18×10^{43}	2.7×10^{47}
				p^+synch	15.92×10^{-8}	1.35×10^{47}	
$K_{11.1}$	9.93×10^{-8}	10^{21}	8.42×10^{46}	e^-synch	9×10^{-12}	7.63×10^{42}	1.68×10^{47}
				p^-synch	9.93×10^{-8}	8.42×10^{46}	
$K_{15.7}$	10.7×10^{-8}	10^{21}	9.07×10^{46}	e^-synch	1.4×10^{-11}	1.18×10^{43}	1.8×10^{47}
				p^+synch	10.7×10^{-10}	9.07×10^{46}	

Table 3

Parameters used for modelling multi-wavelength data from extended jet of PKS 1136-135 using broken power law synchrotron emission model for different knots.

Knots	Dist	Γ	θ_{obs}	δ	$B(mG)$	Emission	$E_{min}eV$	$E_{max}eV$	$E_{break}eV$	p_1	p_2
α	$2.7''$	3	5°	5.48	2	e^-synch	3.16×10^6	7.94×10^{10}	5.49×10^6	1.5	2.5
						p^+synch	10^{17}	10^{18}	6.6×10^{17}	1.5	2.5
A	$4.6''$	3	5°	5.48	1.4	e^-synch	3.16×10^6	6.3×10^{10}	6.3×10^6	1.5	2.5
						p^+synch	10^{17}	10^{18}	6.16×10^{17}	1.5	2.5
B	$6.5''$	3	5°	5.48	1.8	e^-synch	3.16×10^6	7.94×10^{10}	3.8×10^6	1.65	2.65
						p^+synch	10^{17}	10^{18}	7.94×10^{17}	1.65	2.65
C	$7.7''$	3	5°	5.48	1.45	e^-synch	3.16×10^6	5.62×10^{10}	5.88×10^7	1.8	2.8
						p^+synch	10^{17}	10^{18}	6.30×10^{17}	1.8	2.8
D	$8.6''$	3	5°	5.48	1.25	e^-synch	3.16×10^6	5.49×10^{10}	7.94×10^6	1.8	2.8
						p^+synch	10^{17}	10^{18}	5.49×10^{17}	1.8	2.8
E	$9.3''$	3	5°	5.48	1.1	e^-synch	3.16×10^6	4.46×10^{10}	1.02×10^7	1.8	2.8
						p^+synch	10^{17}	10^{18}	4.78×10^{17}	1.8	2.8
HS	$10.3''$	3	5°	5.48	1.05	e^-synch	3.16×10^6	4.46×10^{10}	1.12×10^7	1.9	2.9
						p^+synch	10^{17}	10^{18}	4.57×10^{17}	1.9	2.9

Table 4

Particles and magnetic energy densities of different knots and their contribution to jet power for object PKS 1136-135.

Knots	$u'_B(erg/cm^3)$	R cm	P_B(erg/sec)	Emission	$u'_{part}(erg/cm^3)$	P_{part}(erg/sec)	P_{total}(erg/sec)
α	8.95×10^{-8}	10^{21}	7.59×10^{46}	$e^- synch$	1.6×10^{-12}	1.35×10^{42}	1.51×10^{47}
				$p^+ synch$	8.95×10^{-8}	7.59×10^{46}	
A	7.8×10^{-8}	10^{21}	6.61×10^{46}	$e^- synch$	2.2×10^{-12}	1.86×10^{42}	1.32×10^{47}
				$p^+ synch$	7.8×10^{-8}	6.61×10^{47}	
B	12.89×10^{-8}	10^{21}	1.09×10^{47}	$e^- synch$	5×10^{-12}	4.24×10^{42}	2.18×10^{47}
				$p^+ synch$	12.89×10^{-8}	1.09×10^{47}	
C	8.36×10^{-8}	10^{21}	7.09×10^{46}	$e^- synch$	3×10^{-11}	2.54×10^{43}	1.41×10^{47}
				$p^+ synch$	8.36×10^{-8}	7.09×10^{46}	
D	6.21×10^{-8}	10^{21}	5.26×10^{46}	$e^- synch$	5×10^{-11}	4.24×10^{43}	1.05×10^{47}
				$p^+ synch$	6.21×10^{-8}	5.26×10^{46}	
E	4.81×10^{-8}	10^{21}	4.07×10^{46}	$e^- synch$	1.3×10^{-10}	1.1×10^{44}	8.15×10^{46}
				$p^+ synch$	4.81×10^{-8}	4.07×10^{46}	
HS	4.38×10^{-8}	10^{21}	3.71×10^{46}	$e^- synch$	3.4×10^{-10}	2.88×10^{44}	7.44×10^{46}
				$p^+ synch$	4.38×10^{-8}	3.71×10^{46}	

Table 5

Parameters used for modeling multiwavelength data from extended jet of PKS 1229-021 using synchroton emission model for different knots.

Knots	Dist	Γ	θ_{obs}	δ	$B(mG)$	Emission	$E_{min}eV$	$E_{max}eV$	$E_{break}eV$	p_1	p_2
A	$.7''$	3	5°	5.48	4	$e^- synch$	1.58×10^8	5.62×10^{10}	$.77 \times 10^6$	-	2.8
						$p^+ synch$	10^{17}	2×10^{18}	1.73×10^{18}	1.8	2.8
BCD	$1.9''$	3	5°	5.48	4	$e^- synch$	$.63 \times 10^6$	2.95×10^{10}	$.77 \times \times 10^6$	1.6	2.6
						$p^+ synch$	10^{17}	2×10^{18}	1.73×10^{18}	1.6	2.6

Table 6

Particles and magnetic energy densities of different knots and their contribution to jet power for object PKS 1229-021

Knots	$u'_B(erg/cm^3)$	R cm	P_B(erg/sec)	Emission	$u'_{part}(erg/cm^3)$	P_{part}(erg/sec)	P_{total}(erg/sec)
A	6.36×10^{-7}	10^{21}	5.4×10^{47}	$e^- synch$	9×10^{-13}	7.63×10^{41}	1.08×10^{48}
				$p^+ synch$	6.36×10^{-7}	5.4×10^{48}	
BCD	6.36×10^{-7}	10^{21}	5.4×10^{47}	$e^- synch$	10×10^{-11}	8.48×10^{43}	1.08×10^{48}
				$p^+ synch$	6.36×10^{-7}	5.4×10^{48}	

Table 7

Parameters used for modelling multi-wavelength data from extended jet of PKS 1354+195 using broken power law synchrotron emission model for different knots.

Knots	Dist	Γ	θ_{obs}	δ	$B(mG)$	Emission	$E_{min}eV$	$E_{max}eV$	$E_{break}eV$	p_1	p_2
A	$1.7''$	3	5°	5.48	1	$e^- synch$	3.16×10^6	5.24×10^{10}	1.23×10^7	1.5	2.5
						$p^+ synch$	10^{17}	5.01×10^{17}	4.36×10^{17}	1.5	2.5
B	$4''$	3	5°	5.48	0.5	$e^- synch$	3.16×10^6	7.94×10^{10}	4.89×10^7	1.7	2.7
						$p^+ synch$	10^{17}	5.01×10^{17}	2.18×10^{17}	1.7	2.7

Table 8

Particles and magnetic energy densities of different knots and their contribution to jet power for object PKS 1354+195

Knots	$u'_B(erg/cm^3)$	R cm	P_B(erg/sec)	Emission	$u'_{part}(erg/cm^3)$	P_{part}(erg/sec)	P_{total}(erg/sec)
A	3.98×10^{-8}	10^{21}	3.37×10^{46}	e^-synch	5×10^{-11}	4.24×10^{43}	1.72×10^{48}
				p^+synch	2×10^{-6}	1.69×10^{48}	
B	1.99×10^{-8}	10^{21}	1.68×10^{46}	e^-synch	4×10^{-11}	3.39×10^{43}	2.53×10^{47}
				p^+synch	2.8×10^{-7}	2.37×10^{47}	

Table 9

Parameters used for modelling multi-wavelength data from extended jet of PKS 2209+080 using simple power law electron synchrotron emission model spectrum and broken power proton synchrotron emission model of different knots.

Knots	Dist	Γ	θ_{obs}	δ	$B(mG)$	Emission	$E_{min}eV$	$E_{max}eV$	$E_{break}eV$	p_1	p_2
A	$0.52''$	3	5°	5.48	2	e^-synch	3.16×10^8	6.3×10^{10}	3.09×10^6	-	2.8
						p^+synch	10^{17}	10^{18}	8.7×10^{17}	1.8	2.8
B	$1.3''$	3	5°	5.48	1.4	e^-synch	3.16×10^8	7.07×10^{10}	6.3×10^6	-	2.8
						p^+synch	10^{17}	10^{18}	6.16×10^{17}	1.8	2.8
C	$2''$	3	5°	5.48	1.65	e^-synch	3.98×10^8	3.98×10^{10}	4.57×10^6	-	2.8
						p^+synch	10^{17}	10^{18}	7.24×10^{17}	1.8	2.8
D	$3.2''$	3	5°	5.48	1	e^-synch	6.30×10^8	3.16×10^{10}	1.23×10^7	-	2.8
						p^+synch	10^{17}	10^{18}	4.36×10^{17}	1.8	2.8
E	$4.7''$	3	5°	5.48	1.8	e^-synch	3.16×10^8	4.46×10^{10}	3.08×10^6	-	2.8
						p^+synch	10^{17}	10^{18}	7.94×10^{17}	1.8	2.8

Table 10

Particles and magnetic energy densities of different knots and their contribution to jet power for object PKS 2209+080.

Knots	$u'_B(erg/cm^3)$	R cm	P_B(erg/sec)	Emission	$u'_{part}(erg/cm^3)$	P_{part}(erg/sec)	P_{total}(erg/sec)
A	15.92×10^{-8}	10^{21}	1.35×10^{47}	e^-synch	7.5×10^{-13}	6.36×10^{41}	2.7×10^{47}
				p^+synch	15.92×10^{-8}	1.35×10^{47}	
B	7.8×10^{-8}	10^{21}	6.61×10^{46}	e^-synch	7.5×10^{-13}	6.36×10^{41}	1.32×10^{47}
				p^+synch	7.8×10^{-8}	6.61×10^{46}	
C	10.83×10^{-8}	10^{21}	9.18×10^{46}	e^-synch	7.5×10^{-13}	6.36×10^{41}	1.83×10^{47}
				p^+synch	10.83×10^{-8}	9.18×10^{46}	
D	3.98×10^{-8}	10^{21}	3.37×10^{46}	e^-synch	7.5×10^{-13}	6.36×10^{41}	6.74×10^{46}
				p^+synch	3.98×10^{-8}	3.37×10^{46}	
E	12.89×10^{-8}	10^{21}	1.09×10^{47}	e^-synch	7.5×10^{-13}	6.36×10^{41}	2.18×10^{47}
				p^+synch	12.89×10^{-8}	1.09×10^{47}	

Krawczynski H., Hughes S. B. & Horan, D., 2004, **ApJ, 601, 151**
Kusunose M. and Takahara F., 2017, **ApJ, 835, 20**
Mehta, K. T., Georganopoulos, M., Perlman, E. S., Padgett, C. A., & Chartas, G., 2009, **ApJ, 690, 1706**
Meyer, E. T. & Georganopoulos, M., 2014, **ApJ, 780, L27**
Meyer, E.T., Geoganopoulos, M., Sparks, W. B. et al., 2015, **ApJ, 805, 154**
Meyer, E.T., Breiding, P., Georganopoulos, M. et al., 2017, **ApJ, 835, 35**
Nemmen, R. S., Georganopoulos, M., Guiriec, S., et al. 2012, **Science, 338, 1445**
Sambruna, R. M., Maraschi, L., Tavecchio, F., et al., 2002, **ApJ, 571, 206**
Sambruna, R. M., Gambill, J. K., Maraschi, L., et al., 2004, **ApJ, 608, 698**
Sambruna, R. M., Gliozzi, M., Donato, D., et al., 2006, **ApJ, 641, 717**
Sambruna, R. M., Donato, D., Cheung, C. C., Tavecchio, F., & Maraschi, L., 2008, **ApJ, 684, 862**
Simionescu, A.,Stawarz, L., Ichinohe, Y., et al., 2016,**ApJ, 816, L15**
Tavecchio, F., Maraschi, L., Sambruna, R., M., Urry, C. M., 2000, **ApJ, 544, L23**
Tavecchio, F., Maraschi, L., Wolter, A., et al., 2007, **ApJ, 662, 900**
Weisskopf, M. C., Tananbaum, H. D., Van Speybroeck, L. P., & O'Dell, S. L., 2000, **Proc. SPIE, 4012, 2**
Zacharias,M. and Wagner, S. J., 2016, **A & A, 580, 110**

Table 11

Parameters used for modelling multi-wavelength data from extended jet of PKS 0637-752 using synchrotron emission model for different knots.

Knots	Γ	θ_{obs}	δ	$B(mG)$	Emission	$E_{min}eV$	$E_{max}eV$	$E_{break}eV$	p_1	p_2
$WK_{5.7}$	3	4°	5.6	1.5	e^-synch	2×10^6	4.47×10^{10}	5.62×10^6	1.85	2.85
					p^+synch	10^{17}	10^{18}	3.16×10^{17}	1.85	2.85
$WK_{7.8}$	3	4°	5.6	1.5	e^-synch	3.98×10^6	7.94×10^{10}	5.62×10^6	2.1	3.1
					p^+synch	10^{17}	10^{18}	3.16×10^{17}	2.1	3.1
$WK_{8.9}$	3	4°	5.6	1.5	e^-synch	4.78×10^6	6.31×10^{10}	5.62×10^6	2	3
					p^+synch	10^{17}	6.31×10^{17}	3.16×10^{17}	2	3
$WK_{9.7}$	3	4°	5.6	2.66	e^-synch	10^6	5.01×10^{10}	1.78×10^6	2.25	3.25
					p^+synch	10^{17}	6.31×10^{17}	3.16×10^{17}	2.25	3.25

Table 12

Particles and magnetic energy densities of different knots and their contribution to jet power for object PKS 0637-752

Knots	$u'_B(erg/cm^3)$	R cm	P_B(erg/sec)	Emission	$u'_{part}(erg/cm^3)$	P_{part}(erg/sec)	P_{total}(erg/sec)
$WK_{5.7}$	8.95×10^{-8}	10^{21}	7.58×10^{46}	e^-synch	5.35×10^{-11}	4.53×10^{43}	1.22×10^{47}
				p^+synch	5.5×10^{-8}	4.66×10^{46}	
$WK_{7.8}$	8.95×10^{-8}	10^{21}	7.58×10^{46}	e^-synch	2×10^{-10}	1.69×10^{44}	3.51×10^{47}
				p^+synch	3.25×10^{-7}	2.75×10^{46}	
$WK_{8.9}$	8.95×10^{-8}	10^{21}	7.58×10^{46}	e^-synch	1.1×10^{-10}	9.32×10^{43}	3.73×10^{47}
				p^+synch	3.5×10^{-7}	2.97×10^{47}	
$WK_{9.7}$	2.81×10^{-7}	10^{21}	2.38×10^{47}	e^-synch	5.25×10^{-10}	4.45×10^{44}	3.19×10^{47}
				p^+synch	9.5×10^{-8}	8.05×10^{46}	